Multi-Scale Spiking Network Model of Human Cerebral Cortex

Jari Pronold[1,2], Alexander van Meegen[1,3], Renan O. Shimoura[1], Hannah Vollenbröker[1,4],
Mario Senden[5,6], Claus C. Hilgetag[7], Rembrandt Bakker[1,8], Sacha J. van Albada[1,3]

[1] Advanced Simulation (IAS-6), Jülich Research Centre, Jülich, Germany
[2] RWTH Aachen University, Aachen, Germany
[3] Institute of Zoology, University of Cologne, Cologne, Germany
[4] Heinrich Heine University Düsseldorf, Düsseldorf, Germany
[5] Department of Cognitive Neuroscience, Faculty of Psychology and Neuroscience, Maastricht University, Maastricht, The Netherlands
[6] Maastricht Brain Imaging Centre, Faculty of Psychology and Neuroscience, Maastricht University, Maastricht, The Netherlands
[7] Institute of Computational Neuroscience, University Medical Center Eppendorf, Hamburg University, Hamburg, Germany
[8] Donders Institute for Brain, Cognition and Behavior, Radboud University Nijmegen, 6525 EN Nijmegen, The Netherlands

Contact: s.van.albada@fz-juelich.de
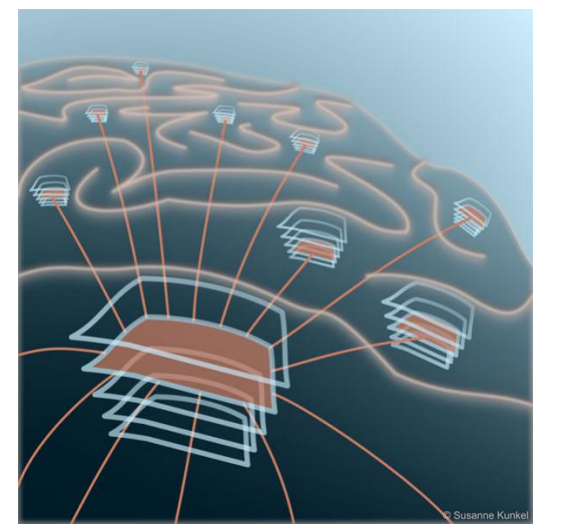
Summary

- We previously created a large-scale spiking network model of all vision-related areas in one hemisphere of macaque cortex [1, 2].

- Building on top of the framework, we have developed a spiking point-neuron network model of the areas in one hemisphere of human cortex [3].

- Model features:

  – Integrates data on cortical architecture such as laminar thicknesses and neuron densities [4, 5], single-cell properties [6], and local [7] and cortico-cortical connectivity [8, 9] into a consistent multi-scale framework.

  – Full neuron [4] and synapse density [10], totaling 3.5 million neurons and 43 billion synapses.

  – Relates cortical network structure to resting-state activity of neurons, populations, layers, and areas.

  – Simulated on a supercomputer using NEST.

  – Compared against experimental spiking data recorded in medial frontal cortex in epileptic patients [11] and whole brain fMRI scans.
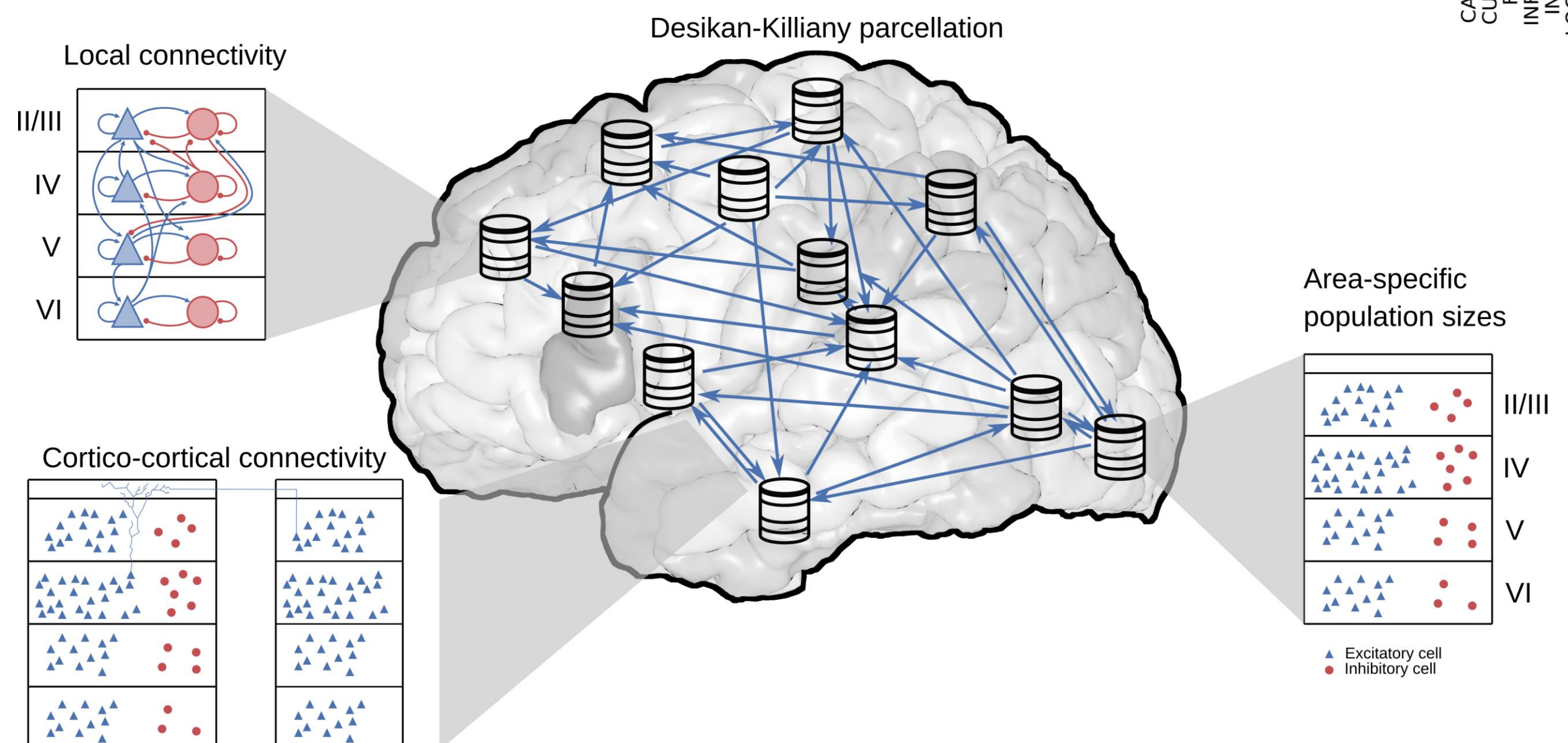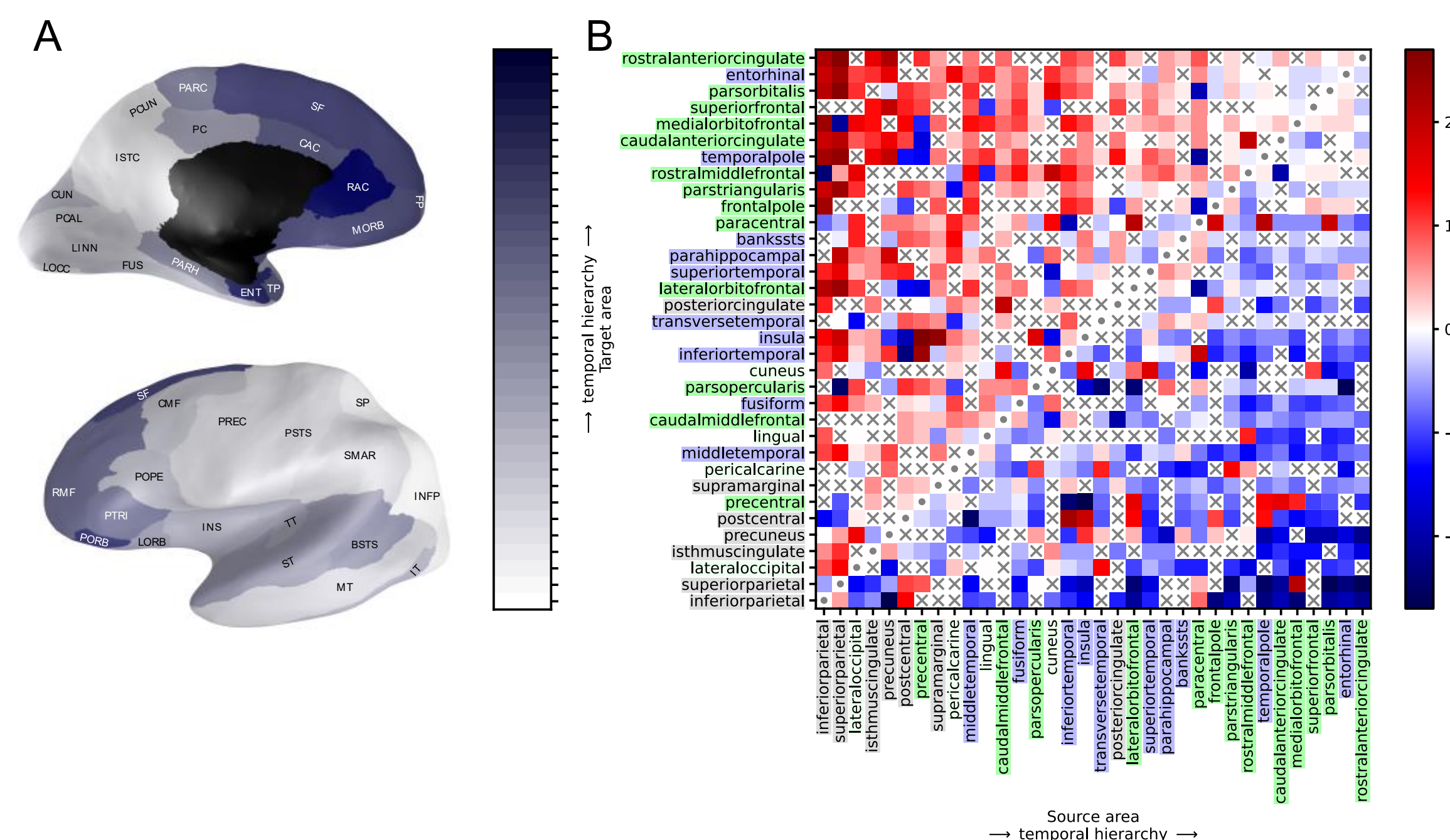
Model parameters
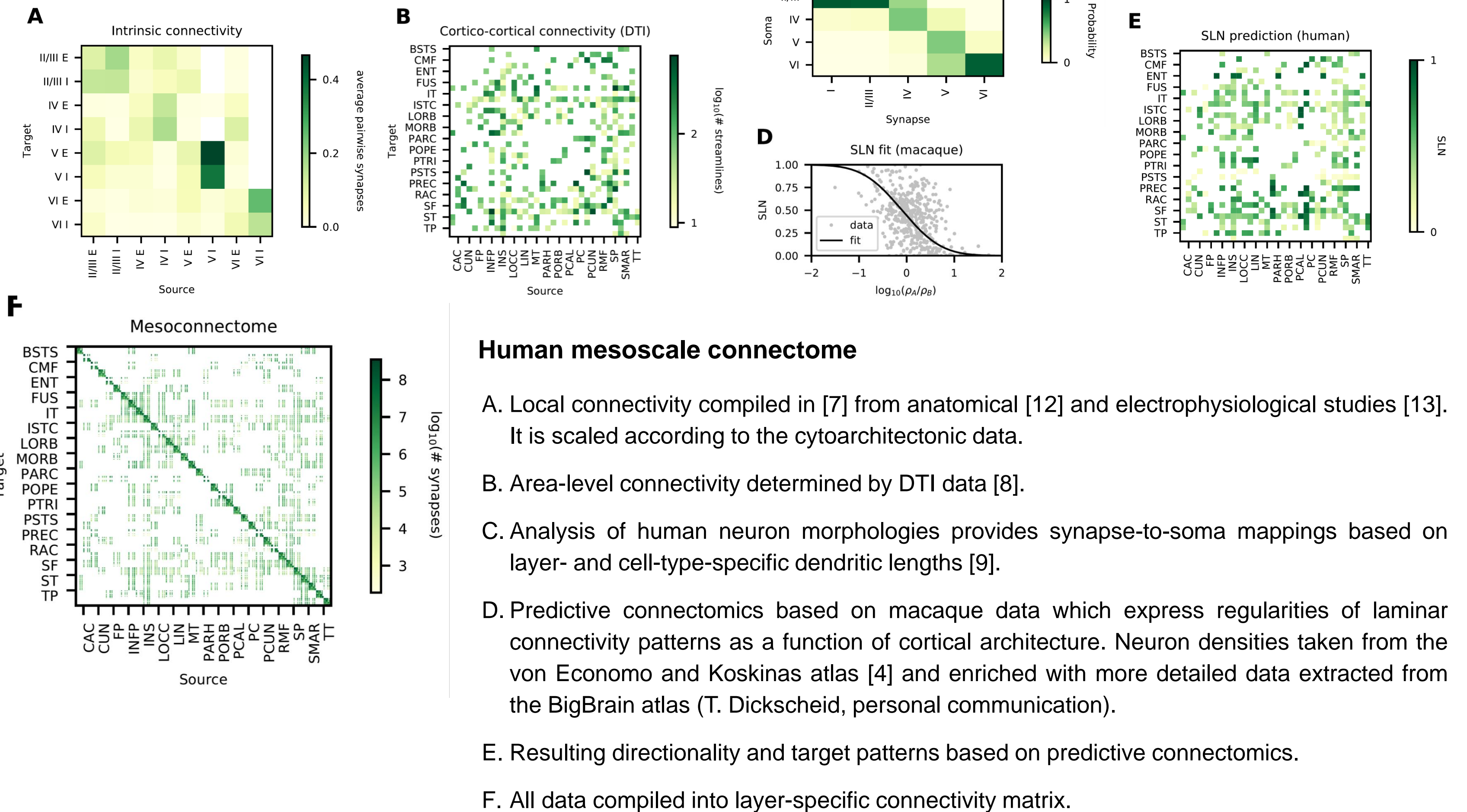
Human mesoscale connectome

A. Local connectivity compiled in [7] from anatomical [12] and electrophysiological studies [13]. It is scaled according to the cytoarchitectonic data.

B. Area-level connectivity determined by DTI data [8].

C. Analysis of human neuron morphologies provides synapse-to-soma mappings based on layer- and cell-type-specific dendritic lengths [9].

D. Predictive connectomics based on macaque data which express regularities of laminar connectivity patterns as a function of cortical architecture. Neuron densities taken from the von Economo and Koskinas atlas [4] and enriched with more detailed data extracted from the BigBrain atlas (T. Dickscheid, personal communication).

E. Resulting directionality and target patterns based on predictive connectomics.

F. All data compiled into layer-specific connectivity matrix.

Connectivity validation
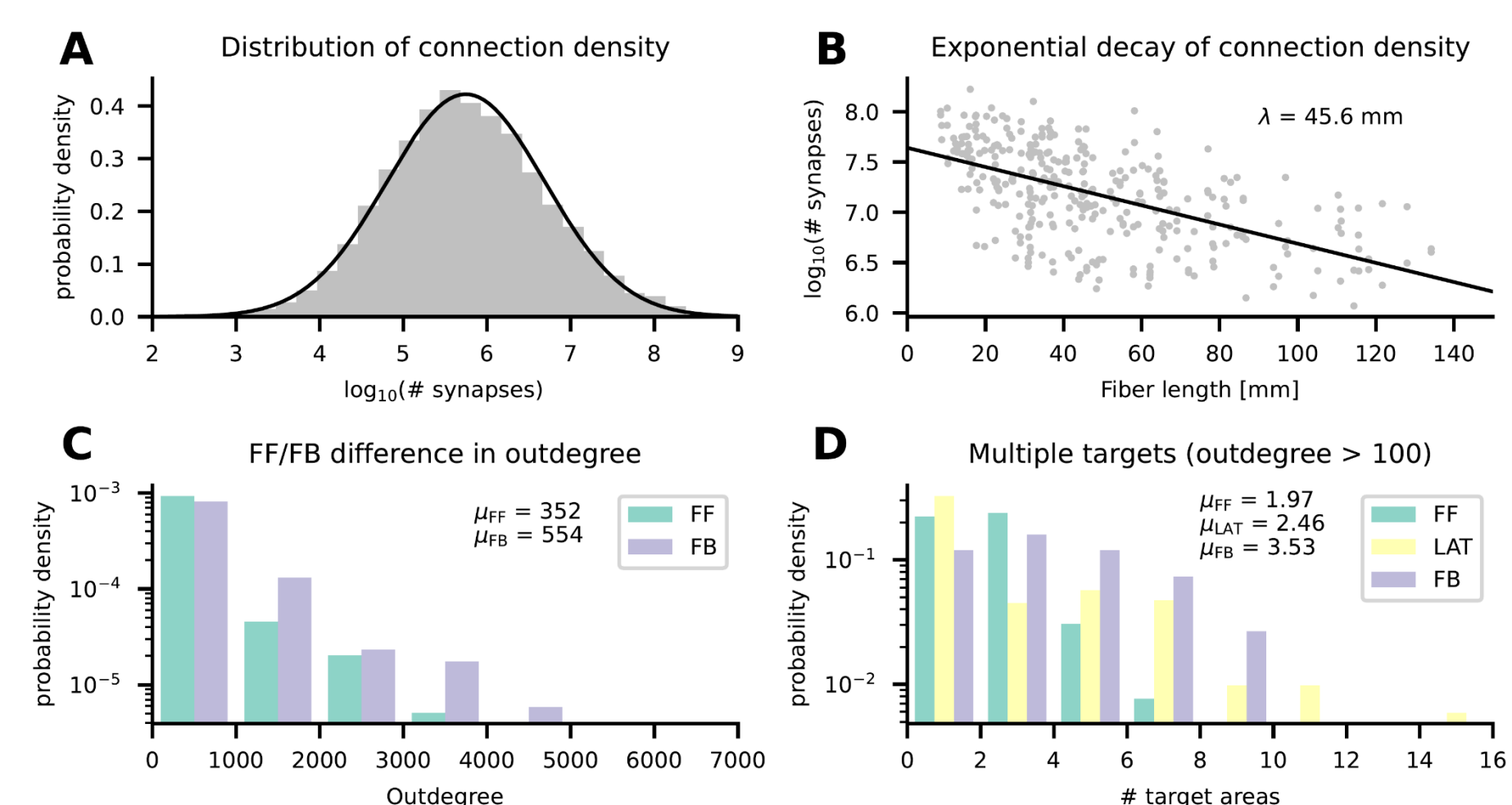
- A-B: Inter-area connection density is log-normally distributed, and it decays exponentially with distance. Similar results found in mouse [15,16], marmoset [17], and macaque [18] data.

- C-D: Feedback projections have larger outdegrees [19], and target more areas on average than feedforward and lateral projections.

Influence of cortico-cortical scaling

Scaling of cortico-cortical connections and experimental data

- A: shows the dependence of different similarity measures on the cortico-cortical scaling factor χ.

- A sudden increase in the similarity of spiking irregularity to experimental data is seen at $\chi = 2.5$.

- B-D: state with $\chi = 2.5$ matches the experimental data better than the ground state, as shown by the firing rate distribution and the CV and LvR [14] statistics.

- E-G: functional connectivities of the experimental and best-fit states show clear structure, while the ground state shows weak correlation and no structure.

Ground state ($\chi = 1.0$)

- Network activity across populations, layers and areas is asynchronous and irregular.
- Inhibitory neurons show higher firing rates than excitatory neurons, CV ≈ 0.8, average pairwise correlation close to zero.

Best-fit state ($\chi = 2.5$)

- Network activity in best-fit state varies across areas, generally higher firing rates than ground state.
- Inhibitory neurons have higher firing rates than excitatory neurons, CV ranges from 0.5 to 1.2, pairwise correlation ranges from 0 to 0.7.
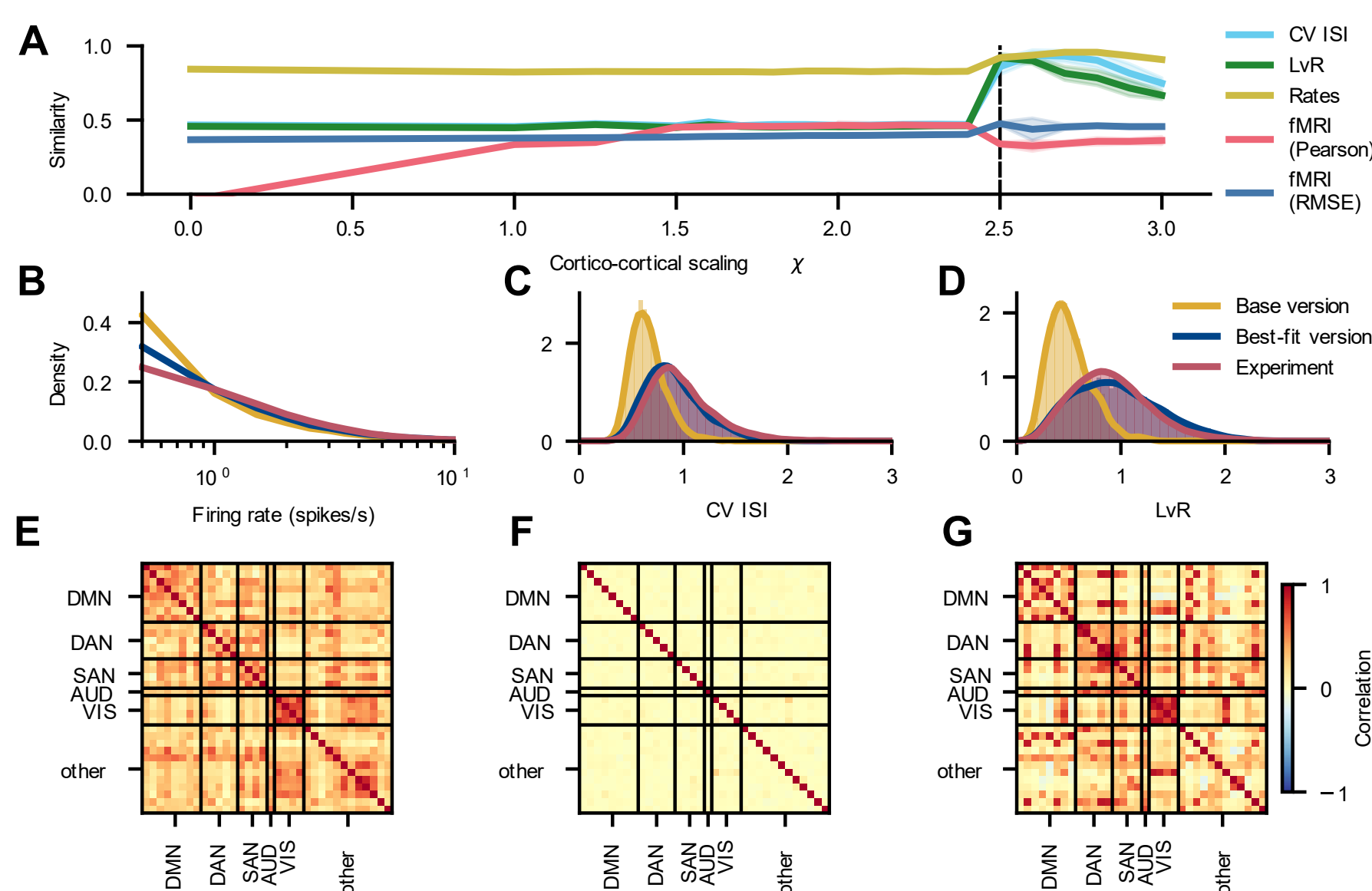
Temporal hierarchy

- Temporal hierarchy of activity flow across the network. Inflated medial and lateral views of the brain (A) depict the temporal order of activation, with colors ranging from white for the most leading area to dark blue for the last. The black zone in the medial view is not part of the model.
- The temporal hierarchy matrix in (B) is based on the estimation of delays obtained as peaks in the cross-correlation function between source and target area, with ordering based on hierarchical clustering. Cells marked with "x" indicate delays classified as 'undecided'. On the x- and y-axis the brain area labels are colored according to a coarse anatomical division of parietal (gray), occipital (light gray), temporal (blue) and frontal (green) lobes.
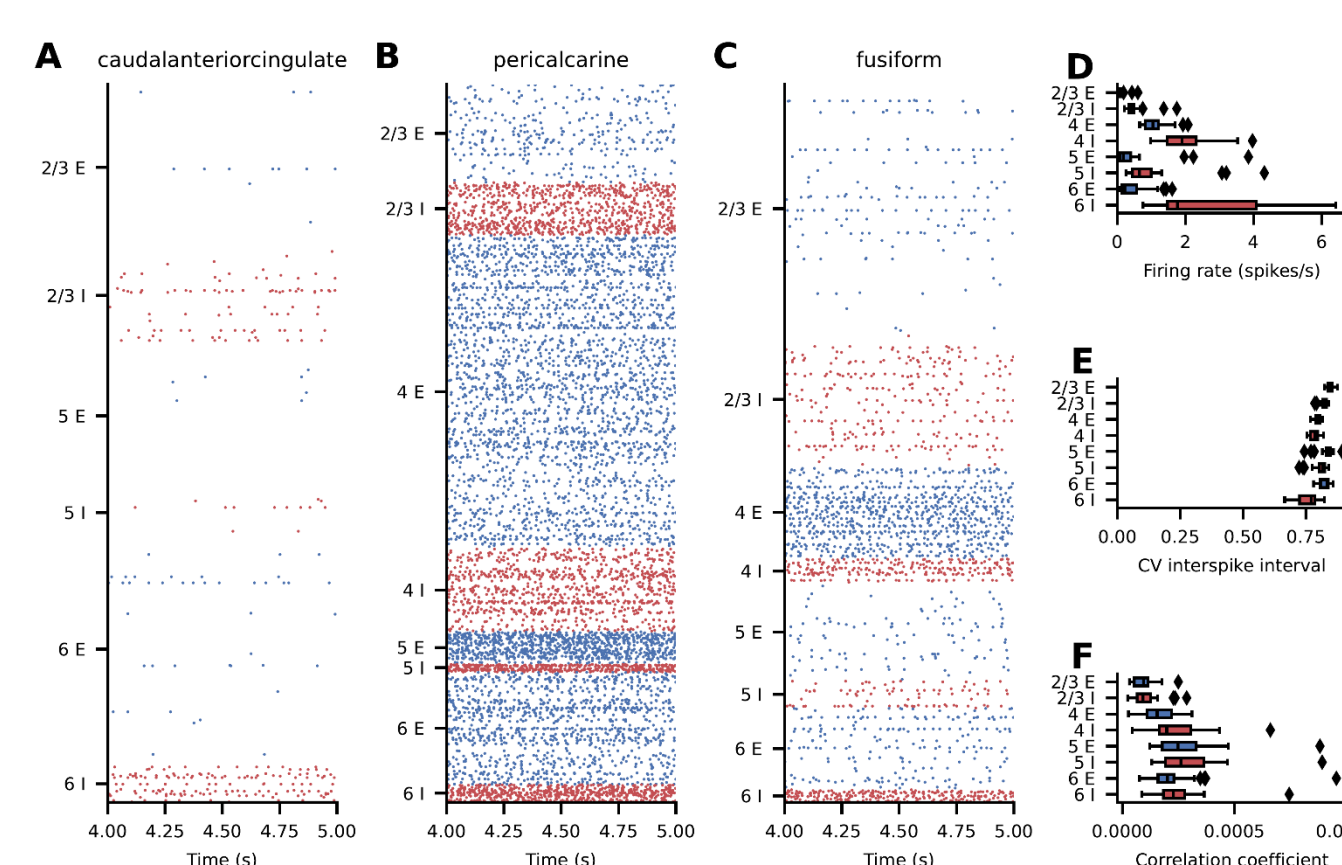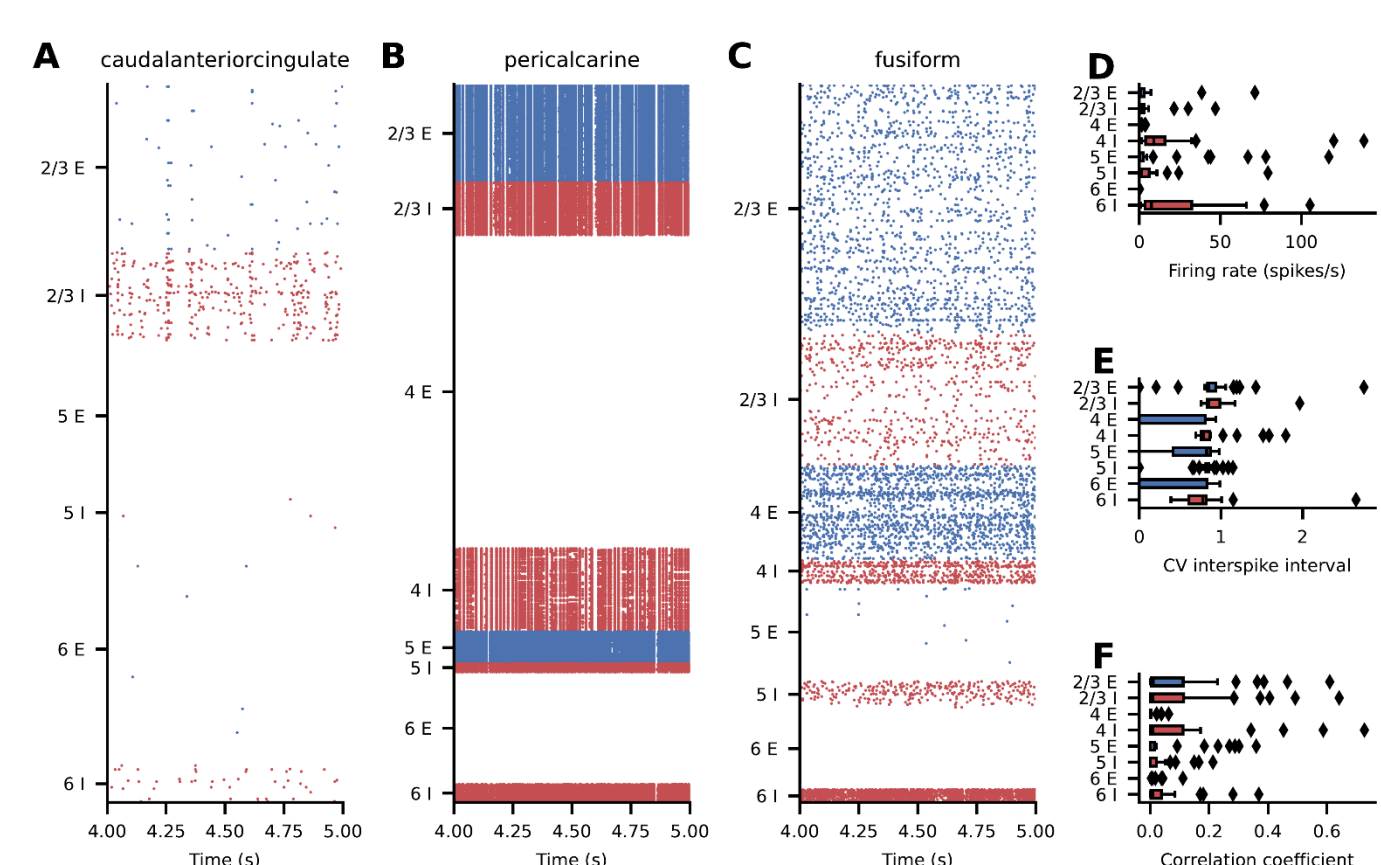
References

[1] Schmidt M, Bakker R, Hilgetag C-C, Diesmann M, van Albada SJ (2018) Brain Struct Func 223(3): 1409-1435.

[2] Schmidt M, Bakker R, Shen K, Bezgin G, Diesmann M et al. (2018) PLOS CB 14(10): e1006359.

[3] Pronold, J., Meegen, A. van, Vollenbröker, H., Shimoura, R. O., Senden, M., et al. (2023).

[4] von Economo CF, Koskinas GN, Triarhou LC (2008) Karger.

[5] Wagstyl K, Larocque S, Cucurull G, Lepage C, Cohen JP et al. (2020) PLOS Biol 18(4), e3000678.

[6] Eyal G, Verhoog MB, Testa-Silva G., Deitcher Y, Lodder JC et al. (2016) Elife 5, p.e16553.

[7] Potjans TC, Diesmann M (2014) Cereb Cortex 24 (3): 785-806.

[8] Van Essen DC, Smith SM, Barch DM, Behrens TEJ, Yacoub E, Ugurbil K (2013) NeuroImage 80:62–79.

[9] Mohan H, Verhoog MB, Doreswamy KK, Eyal G, Aardse R et al. (2015) Cereb Cortex 25(12): 4839-4853.

[10] Cano-Astorga N, DeFelipe J, Alonso-Nanclares L (2021) Cerebral Cortex, 31(10), 4742–4764.

[11] Minxha J, Adolphs R, Fusi S, Mamelak AN, Rutishauser U (2020) Science 368(6498).

[12] Binzegger T, Douglas RJ, Martin KAC (2004) J Neurosci 39: 8441.

[13] Thomson AM, Lamy C (2007) Front Neurosci 1: 19.

[14] Shinomoto S, Kim H, Shimokawa T, Matsuno N, Funahashi S et al. (2009) PLOS CB 5(7), p.e1000433.

[15] Gămănuţ R, Kennedy H, Toroczkai Z, Ercsey-Ravasz M, Van Essen DC et al. (2018) Neuron 97(3):698–715.

[16] Horvát S, Gămănuţ, R, Ercsey-Ravasz M, Magrou L, Gămănuţ, B et al. (2016) PLOS Biol. 07; 14(7):1–30.

[17] Theodoni P, Majka P, Reser DH, Wójcik DK, Rosa MGP et al. (2021) Cereb Cortex 07; 32(1):15–28.

[18] Ercsey-Ravasz M, Markov NT, Lamy C, Essen DCV, Knoblauch K et al. (2013) Neuron 80(1):184–197.

[19] Rockland KS (2019) Neuroimage 197:772–784.

[20] Zilles K, & Palomero-Gallagher N (2017) Frontiers in Neuroanatomy, 11, 78.

[21] Murray J D, Bernacchia A, Freedman D J, Romo R, Wallis J D et al. (2014) 17:12, 17(12), 1661–1663.

[22] Duarte R, Seehofer A, Zilles K, Morrison A (2017) Curr Opin Neurobiol. 43:156–165.

[23] Gao R, van den Brink RL, Pfeffer T, Voytek B (2020) eLife 9:e61277

Outlook

We further plan to enhance the model with the most recent updates from the Jülich brain atlas (julich-brain-atlas.de): detailed neuron density estimates and receptor densities of AMPA, NMDA, and GABA-A receptors [20]. These can help to account for the experimentally observed hierarchy of intrinsic timescales across cortex [21] and differential timescales of feedforward and feedback processing [22, 23].

Code and scripts to regenerate the figures on this poster are available on https://github.com/INM-6/human-multi-area-model. This repository also contains a direct link to run a downscaled version of the model on EBRAINS.